Journal of Molecular Structure 1026 (2012) 117–126

Contents lists available at SciVerse ScienceDirect

Journal of Molecular Structure

journal homepage: www.elsevier.com/locate/molstruc

N′-(2-methoxy-benzylidene)-N-[4-(3-methyl-3-phenyl-cyclobutyl)-thiazol-2-yl]-chloro-acetic hydrazide: X-ray structure, spectroscopic characterization and DFT studies

Ersin İnkaya [a,*], Muharrem Dinçer [a], Öner Ekici [b], Alaaddin Cukurovali [b]

[a] Department of Physics, Faculty of Arts and Sciences, Ondokuz Mayıs University, Kurupelit, 55139 Samsun, Turkey
[b] Department of Chemistry, Faculty of Science Fırat University, 23200 Elazığ, Turkey

HIGHLIGHTS

- IR-NMR spectroscopy and X-ray single crystal diffraction.
- Cyclobutane, DFT(B3LYP)/6-311G(d,p).
- Non-linear optical properties of the title compound have been calculated.

ARTICLE INFO

Article history:
Received 7 February 2012
Received in revised form 23 May 2012
Accepted 23 May 2012
Available online 31 May 2012

Keywords:
X-ray structure determination
IR and NMR spectroscopy
DFT calculations
Cyclobutane
Non-linear optical properties

ABSTRACT

In this work, the structure of N′-(2-methoxy-benzylidene)-N-[4-(3-methyl-3-phenyl-cyclobutyl)-thiazol-2-yl]-chloro-acetic hydrazide, ($C_{24}H_{24}ClN_3O_2S$), was characterized by X-ray single crystal diffraction technique, IR-NMR spectroscopy and quantum chemical computational methods as both experimental and theoretically. The compound crystallizes in the orthorhombic space group $P\ na2_1$ with $a = 14.4170\ (4)$ Å, $b = 11.5441\ (4)$ Å, $c = 27.8420\ (8)$ Å and $Z = 8$. X-ray study shows that crystal has two independent molecules in the asymmetric unit. The molecular geometry was also optimized using density functional theory (DFT/B3LYP) method with the 6-311G(d,p) basis set and compared with the experimental data. To determine conformational flexibility, molecular energy profile of the tittle compound was obtained by semi-empirical (AM1) with respect to selected degree of torsional freedom, which was varied from −180° to +180° in steps 10°. From the optimized geometry of the molecule, vibrational frequencies, gauge-independent atomic orbital (GIAO) ^1H and ^{13}C NMR chemical shift values, molecular electrostatic potential (MEP) distribution, non-linear optical properties, frontier molecular orbitals (FMOs) of the title compound have been calculated in the ground state theoretically.

© 2012 Elsevier B.V. All rights reserved.

1. Introduction

The chemistry of aminothiazoles and their derivatives has attracted the attention of chemists, because they exhibit important biological activity in medicinal chemistry [1], such as antibiotic, anti-inflammatory, antihelmintic, or fungicidal properties [2–4]. 2-Aminothiazoles are known mainly as biologically active compounds with a broad range of activities and as intermediates in the synthesis of antibiotics, well-known sulfa drugs, and some dyes [5,6]. In addition, it has been shown that 3-substituted cyclobutane carboxylic acid derivatives exhibit anti-inflammatory and antidepressant activities [7] and also liquid crystal properties [8].

Azomethines (known as Schiff-bases), having imine groups (CH=N) and benzene rings in the main chain alternately, and being π-conjugated, exhibit interest as materials for wide spectrum applications, particularly as corrosion inhibitors [9], catalyst carriers [10,11], thermo-stable materials [12–14], a metal ion complexing agents [15] and in biological systems [16–18]. The Schiff base compounds have been also under investigation during last years because of their potential applicability in optical communications and many of them have NLO behavior [19,20].

Due to the developments in computational chemistry over the past decade, research into the theoretical modeling of drug design, functional material design, etc., has become much more mature. Many important chemical and physical properties of biological and chemical systems can be predicted from first principles using various computational techniques [21]. In recent years, density functional theory (DFT) has been a shooting star in theoretical modeling. The development of better and better exchange–correlation functional has made it possible to calculate many molecular properties with accuracy comparable to traditional correlated *ab*

* Corresponding author. Tel.: +90 362 3121919/5256; fax: +90 362 4576081.
E-mail address: ersin.inkaya@oposta.omu.edu.tr (E. İnkaya).

0022-2860/$ - see front matter © 2012 Elsevier B.V. All rights reserved.
http://dx.doi.org/10.1016/j.molstruc.2012.05.059

initio methods, at more favorable computational cost [22]. A survey of the literature revealed that DFT has great accuracy in reproducing the experimental values for the geometry, dipole moment, vibrational frequency, etc. [23–29].

In this paper, we report the synthesis, characterization and crystal structure of *N′*-(2-methoxy-benzylidene)-*N*-[4-(3-methyl-3-phenyl-cyclobutyl)-thiazol-2-yl]-chloro-acetic hydrazide, ($C_{24}H_{24}ClN_3O_2S$), as well as theoretical studies using the DFT/B3LYP/6-311G(d,p) method. The aim of the present work was to describe and characterize the molecular structure, vibrational properties and chemical shifts of the title compound, both experimentally and theoretically. A comparison of the experimental and theoretical spectra can be very useful in making correct assignments and understanding the basic chemical shift-molecular structure relationship. Molecular electrostatic potential (MEP), frontier molecular orbitals (FMOs), conformational flexibility and nonlinear optical properties of the title compound were studied at the B3LYP/6-311G(d,p) level. We also make comparisons between experimental and calculated values.

2. Experimental and theoretical methods

2.1. Experimental

2.1.1. General remarks

The melting points were determined in open capillary tubes on a digital Gallenkamp melting point apparatus and are uncorrected. The IR spectrum of the tittle compound was recorded in the range 4000–400 cm^{-1} using a Mattson 1000 FT-IR spectrometer with KBr pellets. The ^1H and ^{13}C nuclear magnetic resonance (NMR) spectra were recorded on a Varian-Mercury-Plus 400 MHz spectrometer using TMS as internal standard and $CDCl_3$ (chloroform) as solvent.

2.1.2. Synthesis

A solution of 0.3775 g (1 mmol) of *N*-(2-methoxybenzylidene)-*N′*-[4-(3-methyl-3-phenyl-cyclobutyl)-thiazol-2-yl]-hydrazine was dissolved in 20 mL 1,4-dioxane containing 1 mmol triethylamine. To this solution, 90 μL (1 mmol) chloro acetyl chloride in 10 mL 1,4-dioxane was added dropwise for 2-h period at the room temperature with stirring. The compound thus precipitated was filtered, washed with copious water, and crystallized from ethanol. The shiny crystals suitable for X-ray analysis was obtained by slow evaporation from its alcoholic solution. Yield: 63% M.p.: 395 K (Fig. 1).

2.1.3. Crystallography

The single-crystal X-ray data were collected on a STOE IPDS II image plate diffractometer at 296 K. Graphite-monochromated Mo Kα radiation (λ = 0.71073 Å) and the *w*-scan technique were used. The structure was solved by direct methods using SHELXS-97 [30] and refined through the full-matrix least-squares method

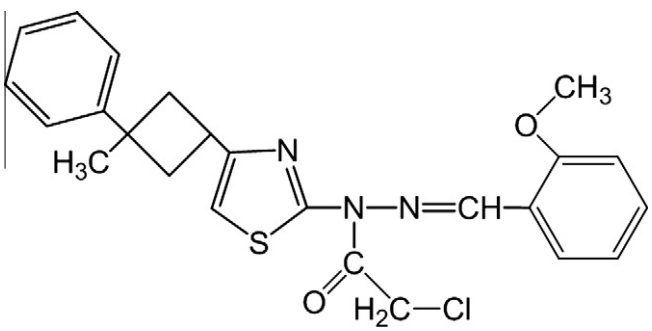

Fig. 1. The structure of the title compound.

Table 1
Crystal data and structure refinement parameters for the title compound.

Color/shape	Light brown
Chemical formula	$C_{24}H_{24}ClN_3O_2S$
Formula weight	453.97
Temperature (K)	296
Wavelength (Å)	0.71073 Mo Kα
Crystal system	Orthorhombic
Space group	$P\,na2_1$
Unit cell parameters	
a, *b*, *c* (Å)	14.4170 (4), 11.5441 (4), 27.8420 (8)
Volume (Å^3)	4633.8 (2)
Z	8
D_{calc} (g/cm^3)	1.302
μ (mm^{-1})	0.28
F(000)	1904
Crystal size (mm^3)	0.78 × 0.49 × 0.11
Diffractometer/measurement method	STOE IPDS 2/ω scan
Index ranges	$-17 \leqslant h \leqslant 17$, $-14 \leqslant k \leqslant 14$, $-33 \leqslant l \leqslant 33$
θ Range for data collection (°)	$1.5 \leqslant \theta \leqslant 25.6$
Reflections collected	32,624
Independent/observed reflections	4469/3266
R_{int}	0.080
Refinement method	Full-matrix least-squares on F^2
Data/restraints/parameters	4469/1/559
Goodness-of-fit on F^2	1.00
R indices [$I > 2\sigma(I)$]	R_1 = 0.0430, wR_2 = 0.0814
R indices (all data)	R_1 = 0.0650, wR_2 = 0.0886
$\Delta\rho_{max}$, $\Delta\rho_{min}$ (e/Å^3)	0.14, −0.13
CCDC deposition no.	815,994

using SHELXL-97 [31], implemented in the WinGX [32] program suite. Non-hydrogen atoms were refined with anisotropic displacement parameters. All H atoms were located in a difference Fourier map and were refined isotropically. Data collection: Stoe X-AREA [33], cell refinement: Stoe X-AREA [33], data reduction: Stoe X-RED [33]. The general-purpose crystallographic tool PLATON [34] was used for the structure analysis and presentation of the results. The structure was refined to R_{int} = 0.080 with 3266 observed reflections using $I > 2\sigma(I)$ threshold. The programs DIAMOND [35] and ORTEP-3 [32] for Windows were used preparation of the figures. Details of the data collection conditions and the parameters of the refinement process are given in Table 1.

2.2. Theoretical

The molecular structure of the compound in the ground state (*in vacuo*) was optimized using density functional theory (DFT/B3LYP) method with the 6-311G(d,p) basis set. All the calculations were performed without specifying any symmetry for the title molecule by using Gauss View molecular visualization program [36] and Gaussian 03 program package [37]. For modeling, the initial guess of the compound was first obtained from the X-ray coordinates. The harmonic vibrational frequencies were calculated at the same level of theory for the optimized structure A and the obtained frequencies were scaled by 0.9669 [38]. The geometry of the compound, together with that of tetramethylsilane (TMS), was fully optimized. ^1H and ^{13}C NMR chemical shifts were calculated using the standard GIAO/B3LYP/6-311G(d,p) (Gauge-Independent Atomic Orbital) approach [39,40] with the Gaussian 03 program package. The predicted ^1H and ^{13}C NMR chemical shifts were derived from the equation $\delta = \Sigma_0 - \Sigma$, where δ is the chemical shift, Σ is the absolute shielding and Σ_0 is the absolute shielding of the standard (TMS), whose values are 31.99 and 184.79 ppm for B3LYP/6-311G(d,p). The effect of solvent on the theoretical NMR parameters was included using the default model IEF-PCM (Integral-Equation-Formalism Polarizable Continuum Model) [41] provided by Gaussian 03. Chloroform was used as solvent.

In order to describe conformational flexibility of the title molecule, the selected torsion angles φ_1 (C6—C1—C7—C9) and φ_2 (S1—C14—N2—N3), was varied from −180° to −180° in every 10° and the molecular energy profile as a function of the selected torsional degree of freedom is obtained by performing single point calculations on the calculated potential energy surface, and the molecular energy profile was obtained at the AM1 calculations. For the calculation of MEP [42,43], the same level theory B3LYP/6-311G(d,p) were used. The mean linear polarisability and mean first hyperpolarisability properties of the title compound were obtained using molecular polarisabilities based on theoretical calculations.

3. Results and discussion

3.1. Crystal structure

The title compound, a DIAMOND view of which is shown in Fig. 2, is a crystallizing in the orthorhombic space group $P\,na2_1$ with eight molecules in unit cell. The asymmetric unit contains two independent molecules (A and B). The tittle molecule composed of a central thiazole ring, with chloro-acetic hydrazide and *N*′-(2-methoxy-benzylidene) groups connected 2-position of the ring and a (3-methyl-3-phenyl-cyclobutyl) group in the 4-position, for both independent molecules.

The thiazole rings are planar with a maximum deviation of 0.0075 (24) Å for atom C13A and −0.0008 (25) Å for atom C13B. In the crystal structure, the phenyl and thiazole rings are in *cis* positions with respect to the cyclobutane ring, for both independent molecules. The dihedral angles between the thiazole planes (S1/N1/C12-C14) with the benzene planes (C1-C6) and the cyclobutane planes (C7, C9-C11) are 74.47°, 37.26° and 88.86°, 48.59°, respectively for molecule A and B. Although close to being planar, the cyclobutane ring is puckered. The C10/C11/C9 plane forms a dihedral angle of 28.08 (5)° with the C9/C7/C10 plane for molecule A and 25.16 (4)° for molecule B. This values is significantly longer than those in the literatures; 23.5 [44], 25.74 (6) [45]. However, when the bond lengths and angles of the cyclobutane rings in the title compound are compared with these, it is seen that there are no significant differences.

There are two obviously different C—N bond distances in the thiazole rings. One of them N1—C14 bond lengths are indicative of a significant double bond character for molecules A and B. Additionally, the C12—C13 bond distances are 1.347 (6) Å and 1.359 (6) Å for both molecules, respectively. According to this results, C12—C13 bonds characterizing a C=C double bond. The S1—C13 and S1—C14 bond lengths are shorter than the accepted value for an S—Csp^2 single bond (1.76 Å; [46]), resulting from the conjugation of the electrons of atom S1 with atoms C13 and C14.

In the molecular structure of the title compound, the interatomic distance between thiophene atom S1 and the carboxyl atom O2 are 2.681 Å and 2.608 Å for both molecules, which are less than the sum of the atomic van der Waals radii for sulfur and oxygen, 1.80 and 1.52 Å, respectively [47]. The directionality of the σ-hole bonds is quite evident; the C—S—O angle is about 159.3°, putting the oxygens approximately on the extension of the C—S bond [48].

Perspective view of the crystal packing in the unit cell is shown in Fig. 3. The crystal structure does not exhibit intermolecular, π–π stacking (face-to-face) interactions. There are, however, one C—H···N intramolecular and one C—H···Cg (π-ring) intermolecular interactions, details of which is given in Table 2. An intramolecular C17—H17···N1 contact leads to the formation of a six-membered ring with graph-set descriptor *S*(6) [49]. In addition, atom C13A at (*x*,*y*,*z*) forms a C—H···Cg (π-ring) contact, *via* atom H13, with the centroid of the C1B—C6B ring. The packing is further stabilized by van der Waals forces.

3.2. Optimized structures

The first task for the computational work is to determine the optimized geometry of the tittle compound. The starting coordinates were those obtained from the X-ray structure determination. The optimized parameters (bond lengths, bond angles and dihedral angles) of the title compound were obtained using the B3LYP/6-311G(d,p) method for both independent molecules. The results are listed in Table 3 and compared with the experimental data for the title compound.

The most notable discrepancies are found in the orientation of the 3-phenyl-cyclobutyl group of the title compound. The

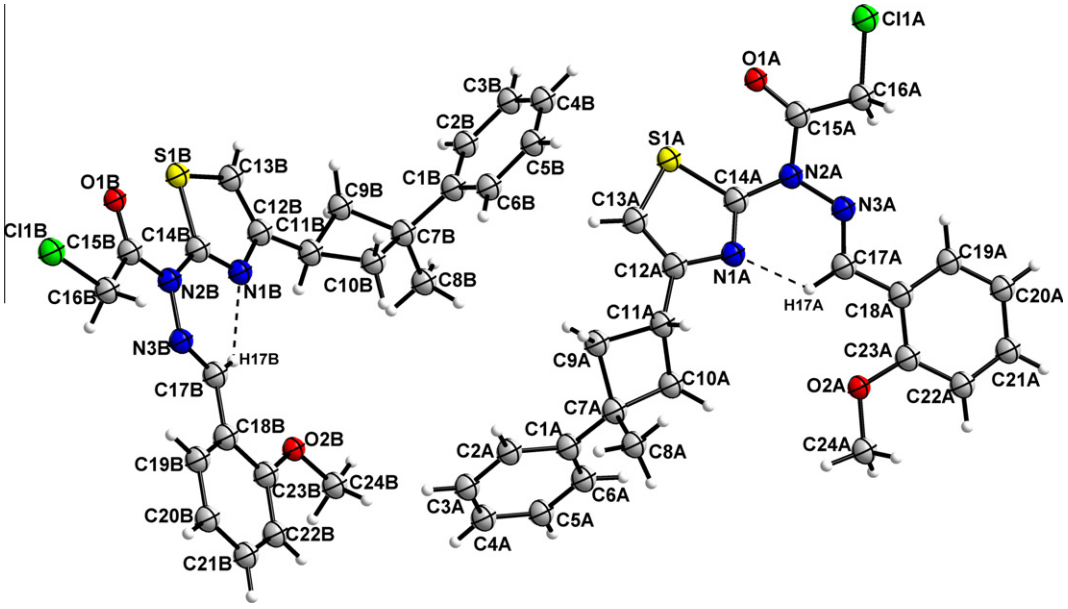

Fig. 2. A view of the title compound showing the atom-numbering scheme. Displacement ellipsoids are drawn at the 40% probability level and H atoms are shown as small spheres of arbitrary radii. Hydrogen bonds are indicated by broken lines.

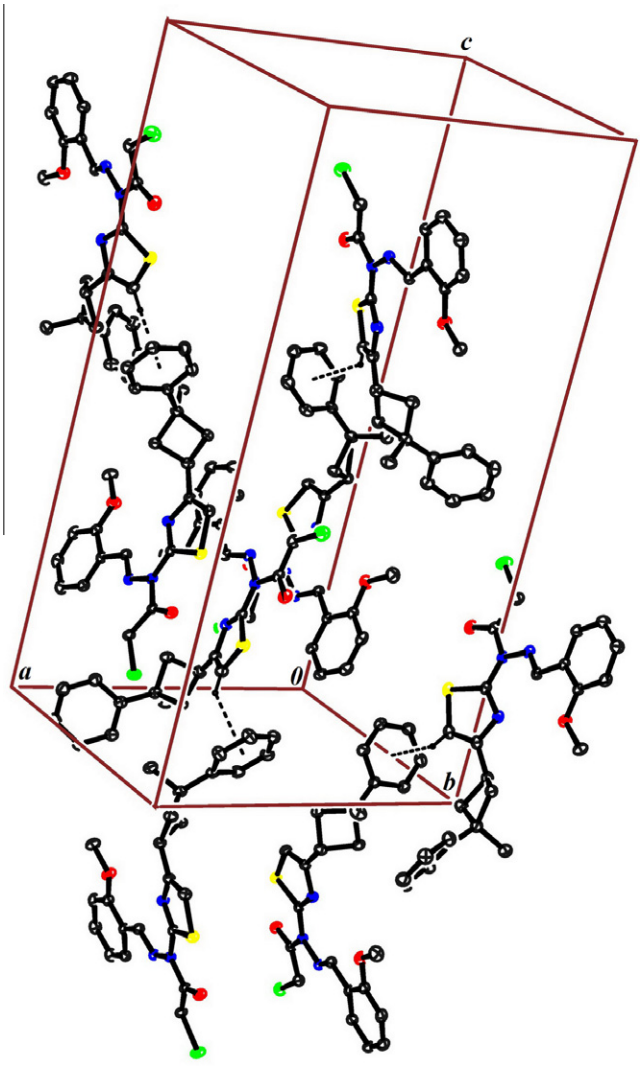

Fig. 3. Packing diagram of the title compound.

Table 2
Hydrogen bonding geometry for the title compound.

D—H···A	D—H (Å)	H···A (Å)	D···A (Å)	D—H···A (°)
C17A—H17A···N1A	0.93	2.21	2.831 (5)	123
C17B—H17B···N1B	0.93	2.08	2.757 (5)	128
C13A—H13···Cg7^{i}	0.93	2.98	3.733	139
B3LYP/6-311G(d,p)				
C17A—H17A···N1A	1.08	2.08	2.80	121.69
C17B—H17B···N1B	1.08	2.08	2.81	121.70

Symmetry code: (i) $-x+1/2, y+1/2, z-1/2$. Cg7: Centroid of the C1B—C6B.

orientation of the 3-phenyl-cyclobutyl group for A and B are defined by a torsion angles C6—C1—C7—C10 of 127.3 (5)° and 127.2 (5)° for the X-ray structure and 141.15° and 141.06° for B3LYP, respectively. The dihedral angles between the thiazole planes (S1/N1/C12-C14) with the benzene planes (C1-C6) and the cyclobutane planes (C7, C9-C11) for the independent molecule A and B are 74.47°, 37.26° and 88.86°, 48.59° in the X-ray structure, and in the optimized structures the corresponding angles are 75.81°, 46.74° and 75.82°, 46.61°, respectively.

As seen from Table 3, most of the optimized bond lengths are slightly longer than the experimental values and the bond angles are slightly different from the experimental angles. We note that

Table 3
Experimental and optimized geometrical parameters of the title compound.

Parameters	Experimental		Calculated B3LYP/6-311G(d,p)	
	A	B	A	B
Bond lengths (Å)				
Cl1—C16	1.771 (4)	1.777 (4)	1.7968	1.7969
N1—C14	1.301 (5)	1.295 (4)	1.2992	1.2993
N2—C15	1.389 (5)	1.382 (4)	1.4052	1.4052
N3—C17	1.269 (4)	1.262 (4)	1.2847	1.2847
O1—C15	1.208 (5)	1.206 (4)	1.2073	1.2074
O2—C23	1.347 (5)	1.349 (5)	1.3614	1.3614
O2—C24	1.429 (5)	1.433 (5)	1.4219	1.4220
S1—C13	1.698 (5)	1.718 (5)	1.7378	1.7379
S1—C14	1.732 (4)	1.734 (3)	1.7674	1.7675
C1—C2	1.379 (7)	1.382 (6)	1.3994	1.3995
C2—C3	1.381 (8)	1.373 (7)	1.3930	1.3930
C3—C4	1.362 (9)	1.339 (7)	1.3929	1.3931
C12—C13	1.347 (6)	1.359 (5)	1.3601	1.3602
Bond angles (°)				
C15—N2—N3	111.8 (3)	112.9 (3)	113.001	113.002
C17—N3—N2	122.3 (3)	121.9 (3)	123.436	123.436
N1—C12—C11	118.4 (4)	117.1 (3)	117.846	117.851
C23—O2—C24	118.6 (3)	118.0 (3)	119.045	119.045
N1—C14—N2	122.2 (3)	123.2 (3)	123.031	123.031
N1—C14—S1	115.5 (3)	114.8 (3)	114.355	122.613
O1—C15—N2	121.5 (4)	121.3 (3)	121.510	121.511
N2—C15—C16	113.7 (3)	114.6 (3)	114.734	114.734
O2—C23—C22	125.4 (3)	125.1 (4)	116.291	116.293
C13—S1—C14	87.9 (2)	88.12 (18)	87.782	87.7825
C10—C7—C9	86.2 (3)	87.3 (3)	87.850	87.8533
C9—C11—C10	87.6 (4)	88.2 (3)	88.610	88.6142
Dihedral angles (°)				
N3—N2—C14—S1	−165.3 (3)	176.6 (3)	−179.458	−179.430
N2—N3—C17—C18	176.8 (3)	178.4 (3)	179.896	179.885
N3—N2—C15—O1	174.6 (4)	−179.6 (4)	179.954	179.941
C13—S1—C14—N2	−179.2 (4)	−179.9 (3)	179.593	179.590

the experimental results are for the solid phase and the theoretical calculations are for the gas phase. In the solid state, the existence of a crystal field along with the intermolecular interactions connect the molecules together, which results in the differences in bond parameters between the calculated and experimental values [50].

A global comparison was performed by superimposing the molecular skeletons obtained from X-ray diffraction and the theoretical calculations atom by atom (Fig. 4), obtaining RMSE values of 0.973 and 1.715 Å for A and B, respectively. According to this result, the smallest RMSE value is obtained for molecule A and the geometry obtained from this molecule coincides better with the crystalline structure than molecule B. For that reason, we used the geometry from molecule A, while calculate other parameters such as vibrational frequencies, molecular electrostatic potential (MEP), frontier molecular orbitals (FMOs) and conformational flexibility.

3.3. Vibrational spectra

It is well known that the calculated harmonic frequencies are usually higher than the corresponding experimental quantities and tend to overestimate vibrational frequencies. After scaling, the error distributions match well with the experimental frequencies and the calculated vibrations are in good agreement with the experimental results. DFT calculations on harmonic frequencies have provided excellent vibrational frequencies for organic compounds if a proper scaling factor is used to correct the calculated frequencies to compensate for the approximate treatment of electron correlation, for the anharmonicity effects and for basis set deficiencies [51]. So, in this work, the theoretical harmonic frequencies have been scaled by the classical factor of 0.9669

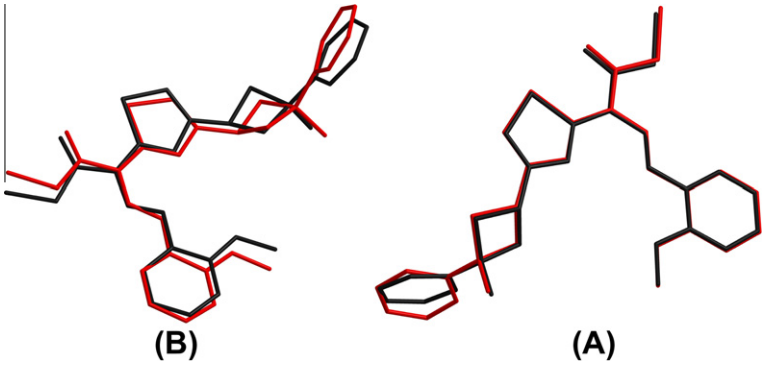

Fig. 4. Atom-by-atom superimposition of the calculated structures (red) on the X-ray structures (black) for molecules A and B.

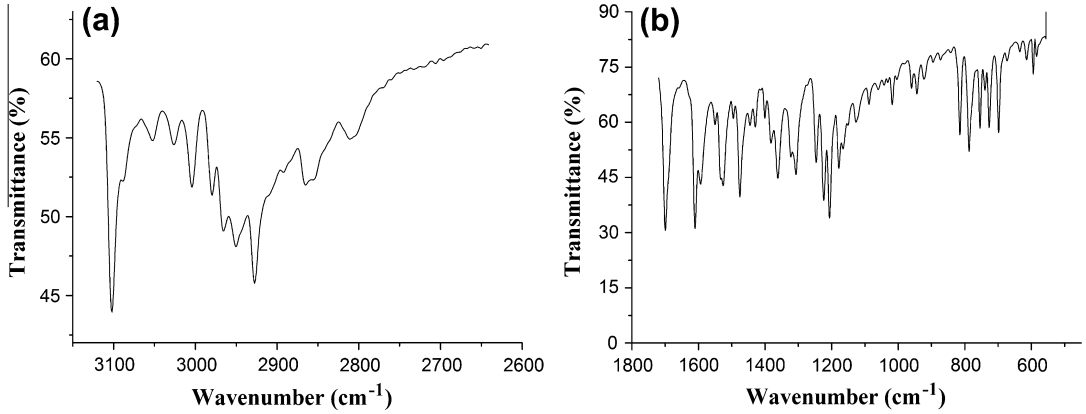

Fig. 5. Experimental FT-IR spectra (a) From 3200 to 2700 cm^{-1} and (b) From 1800 to 500 cm^{-1}.

according to [37] in order to correct the theoretical error. The vibrational bands assignments have been made by using Gauss View molecular visualization program [36].

The experimental and theoretical simulated FT-IR spectra are shown in Figs. 5a and b, and 6a and b, where the experimental and calculated infrared intensities are plotted against the vibrational frequencies. As a whole, the calculated spectra are more regular than the observed FT-IR and some bands found in the predicated IR spectra were not observed in the experimental spectra, as shown in Fig. 4 and Table 4. This is due to the fact that many vibrations presenting in condensed phase lead to strong perturbation of infrared intensities of many other modes.

In the higher frequency region, almost all of the vibrations belong to C—H_3 and ring C—H and C—H_2 stretching vibrations. The C—H, C—H_2 and C—H_3 symmetrical and asymmetrical stretching vibrations are observed at 2649–3104 cm^{-1} range and theoretically these frequencies have been calculated at 2908–3141 cm^{-1} region for B3LYP. Two different *ν*C=N stretching vibrations are appeared in the tittle molecule. One of them is observed at 1612 cm^{-1} band in thiazole ring whereas the other appeared at 1535 cm^{-1} in azomethine group. These bands have been calculated at 1604 and 1518 cm^{-1} for B3LYP/6-311G(d,p), respectively. Another characteristic region of the thiazole derivative spectrum is 1535–1160 cm^{-1}, which is attributed to *ν*C=N and *ν*C—S stretching vibrations. The tittle compound shows a strong band at 1715 cm^{-1} which is assigned to *ν*C=O stretching. The stretching *ν*C=O vibration gives rise to a band in the experimental infrared spectrum at 1715 cm^{-1}, and the calculated value is predicted to be 10 cm^{-1} higher at 1725 cm^{-1}. The other calculated vibrational frequencies can be seen in Table 4.

To make a comparison with experimental observations, we studied the correlation between the calculated and the experimental data, and obtained a correlation coefficient of 0.99617 for B3LYP/6-311G(d,p). As we can see from the correlation graphs in Fig. 6, the experimental fundamentals are found to have a good correlation with the calculations.

3.4. NMR spectra

The characterization of the compound was further enhanced by the use of ^{1}H and ^{13}C NMR spectroscopy. The ^{1}H and ^{13}C NMR spectra of the tittle compound recorded using TMS as an internal standard and chloroform ($CDCl_3$) as solvent. GIAO ^{1}H and ^{13}C chemical shift values (with respect to TMS) were calculated using the B3LYP method with the 6-311G(d,p) basis set and compared with experimental ^{1}H and ^{13}C chemical shift values. The results of this calculation are shown in Table 5 together with the experimental values.

We have calculated ^{1}H chemical shift values (with respect to TMS) of 11.44–1.56 ppm at the B3LYP/6-311G(d,p) level, however, the experimental results were observed to be 9.14–1.59 ppm. In the ^{1}H NMR spectra of the compound, the chemical shift values of C—H_3 protons were observed to be 1.59* (H8*) and 3.66* (H24*) ppm, respectively. These signals have been calculated as 1.56* and 4.02* ppm for B3LYP methods with the 6-311G(d,p) level, respectively. The C—H_2 signals of cyclobutane ring are observed 2.53* and 2.64* ppm while they appeared 2.61* and 2.55* ppm in theoretical calculation. The CH hydrogen of the thiazole ring appears at 6.92 ppm, and is determined computationally at 9.45 ppm. The chemical shift of an azomethine CH=N hydrogen calculated at 9.14 ppm and is observed to be 11.44 ppm in the experimental spectra.

^{13}C NMR spectra of tittle compound show signal at 167.57 and 159.05 ppm, respectively, due to the C14 and C15 atoms of thiazole and carboxyl groups. These signals were calculated at 166.16 and

Table 4
Comparison of the observed and calculated vibrational spectra of the title compound.

Assignment	Experimental IR with KBr (cm^{-1})	Calculated (cm^{-1}) B3LYP/6-311G(d,p)	
		Scaled freq.	*I* (km/mol)
$\nu C—H_{(thiazole)}$	3104	3141	1.25
$\nu C—H_{(azomethine)}$	–	3113	12.30
$\nu_s C—H_{(phenyl)}$	–	3105	9.70
$\nu_{as} C—H_{(phenyl)}$	3057	3097	11.32
$\nu_s C—H_{(phenyl)}$	–	3082	21.90
$\nu_{as} C—H_{(phenyl)}$	3025	3081	16.18
$\nu_{as} C—H_{(phenyl)}$	–	3071	35.53
$\nu_{as} C—H_{(phenyl)}$	–	3064	10.16
$\nu_{as} C—H_{2(chl.\ act.\ acid)}$	–	3063	1.04
$\nu_{as} C—H_3$	–	3034	18.10
$\nu_s C—H_{2(chl.\ act.\ acid)}$	2963	3010	15.75
$\nu_{as} C—H_{2(cyclobutane)}$	2960	3003	33.36
$\nu_{as} C—H_3$	–	2982	52.61
$\nu_{as} C—H_3$	–	2967	33.31
$\nu_s C—H_{2(cyclobutane)}$	–	2945	38.94
$\nu C—H_{(cyclobutane)}$	2866	2944	8.58
$\nu_s C—H_3$	2649	2908	59.30
$\nu C{=}O$	1715	1725	292.09
$\nu C{=}N_{(azomethine)} + \nu C—C_{(phenyl)}$	1612	1604	76.46
$\nu C{=}C_{(phenyl)}$	1580	1568	2.04
$\nu C{=}C_{(thiazole)} + \nu C{=}N_{(thiazole)}$	1535	1518	54.12
$\gamma C—H_{(phenyl)} + \alpha C—H_3$	–	1473	117.76
$\gamma C—H_{2(cyclobutane)} + \alpha C—H_3$	1500	1454	24.25
$\alpha C—H_3$	–	1446	2.33
$\alpha C—H_{2(chl.\ act.\ acid)}$	1430	1394	14.36
$\alpha C—H_{(azomethine)}$	–	1371	9.45
$\gamma C—H_{(cyclobutane)}$	1365	1342	3.83
$\omega C—H_{2(chl.\ act.\ acid)} + \nu C—N$	–	1296	109.84
$\omega C—H_{2(cyclobutane)} + \nu C—C$	1270	1278	40.23
$\nu C—N_{(thiazole)} + \alpha C—H_{2(chl.\ act.\ acid)}$	–	1256	37.11
$\nu C—O—C$	1200	1235	249.90
$\nu C—N—N + \nu C—S$	1160	1212	247.69
$\gamma C—H_{(phenyl)}$	1075	1147	17.58
$\delta C—H_{2(chl.\ act.\ acid)}$	–	1145	0.78
$\delta C—H_{2(cyclobutane)} + \gamma C—H_{(thiazole)}$	–	1135	14.61
$\nu C—O + \theta_{(phenyl)}$	960	1020	34.20
$\nu C—N_{(thiazole)} + \gamma C—H_{(thiazole)}$	–	1010	7.80
$\beta C—H_{(azomethine)}$	–	999	7.66
$\nu C—C_{(cyclobutane)}$	–	982	2.41
$\beta C—H_{(phenyl)}$	–	967	0.14
$\theta_{(cyclobutane)}$	940	933	4.66
$\gamma C—H_{2(chl.\ act.\ acid)}$	–	903	7.72
$\nu C—Cl_{(chl.\ act.\ acid)}$	733	780	29.47
$\beta C—H_{(phenyl)}$	–	755	26.66
$\beta C—H_{(phenyl)}$	720	742	64.43
$\beta C—H_{(thiazole)}$	–	723	26.22
$\nu S—C—N_{(thiazole)} + \nu C—C_{(chl.\ act.\ acid)}$	701	707	100.25
$\beta C—H_{(phenyl)}$	644	693	47.60
$\theta_{(thiazole)}$	–	603	7.47
$\beta C—H_{(phenyl)}$	566	538	13.66

Vibrational modes: ν, stretching; α, scissoring; γ, rocking; ω, wagging; δ, twisting; β, in-plane bending; θ, ring breathing. Abbreviations: *s*, symmetric; *as*, asymmetric.

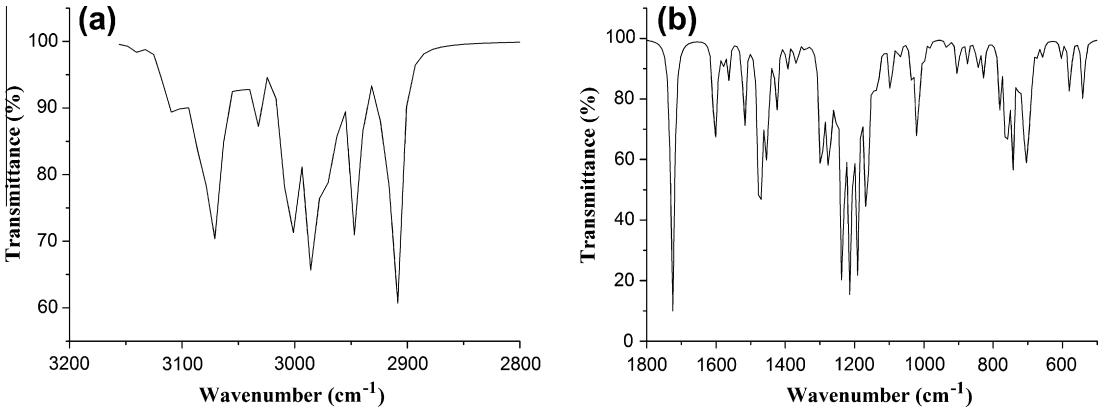

Fig. 6. Theoretical FT-IR spectra (a) from 3200 to 2700 cm^{-1} and (b) from 1800 to 500 cm^{-1}.

Table 5
Experimental and theoretical ^{13}C and ^{1}H isotropic chemical shifts (ppm) for the title compound.

Atom	Experimental (ppm) ($CDCl_3$)	Calculated (ppm) B3LYP/6-311G(d,p)
C1	147.86	160.95
C2	125.02	130.91
C3	126.71	134.39
C4	125.56	131.38
C5	126.71	134.25
C6	125.02	130.64
C7	39.01	45.91
C8	29.72	34.04
C9	41.12	40.57
C10	41.12	46.09
C11	31.11	36.15
C12	152.01	161.15
C13	111.52	117.31
C14	167.57	166.16
C15	159.05	174.37
C16	43.89	56.91
C17	155.60	152.09
C18	121.09	128.71
C19	128.37	131.18
C20	122.08	125.89
C21	132.73	139.66
C22	112.51	114.79
C23	157.15	167.6
C24	55.67	57.01
H2	6.98	7.48
H3	7.02	7.64
H4	7.14	7.48
H5	7.10	7.58
H8[a]	1.59[a]	1.56[a]
H9[a]	2.53[a]	2.61[a]
H10[a]	2.64[a]	2.55[a]
H11	3.81	4.02
H13	6.92	6.78
H16[a]	4.84[a]	5.13[a]
H17	9.14	11.44
H19	7.92	8.25
H20	7.02	7.32
H21	7.26	7.75
H22	6.92	6.99
H24[a]	3.66[a]	4.02[a]

Note: The atom numbering according to Fig. 2 used in the assignment of chemical shifts.
[a] Average.

174.37 ppm, respectively. The existence of the intramolecular hydrogen bond owing to the azomethine (CH=N) atom is confirmed at ~155.60 ppm. Due to this interaction, the experimental and theoretical chemical shift difference for atom C17. The aliphatic CH_2 (C9, C10 and C16) carbons are observed at 41.12 and 43.89 ppm and the C atoms (C8 and C24) of methyl groups are observed at 29.72 and 55.67 ppm, respectively.

To make comparison with experimental observations, we present correlation graphs in Fig. 7 based on the calculations. As can be seen from the correlation graphs, ^{1}H and ^{13}C the correlation coefficients are 0.99069 and 0.96643 for B3LYP, respectively. As can be seen from Table 5, the theoretical ^{1}H and ^{13}C chemical shift results for the title compound are generally closer to the experimental ^{1}H and ^{13}C shift data.

3.5. Molecular electrostatic potential

The molecular electrostatic potential (MEP) is related to the electronic density and is a very useful descriptor in understanding sites for electrophilic attack and nucleophilic reactions as well as hydrogen-bonding interactions [52–54]. The electrostatic potential $V(r)$ are also well suited for analyzing processes based on the "recognition" of one molecule by another, as in drug–receptor, and enzyme-substrate interactions, because it is through their potentials that the two species first "see" each other [55,56]. Being a real physical property $V(r)$ can be determined experimentally by diffraction or by computational methods [57].

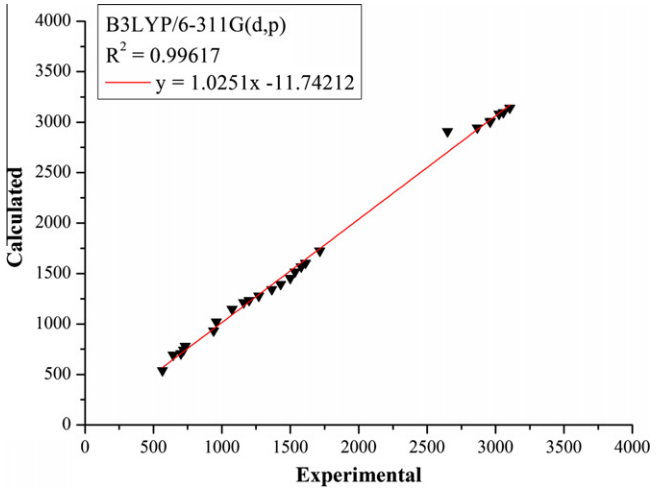

Fig. 7. Correlation graphic of calculated and experimental frequencies of title compound.

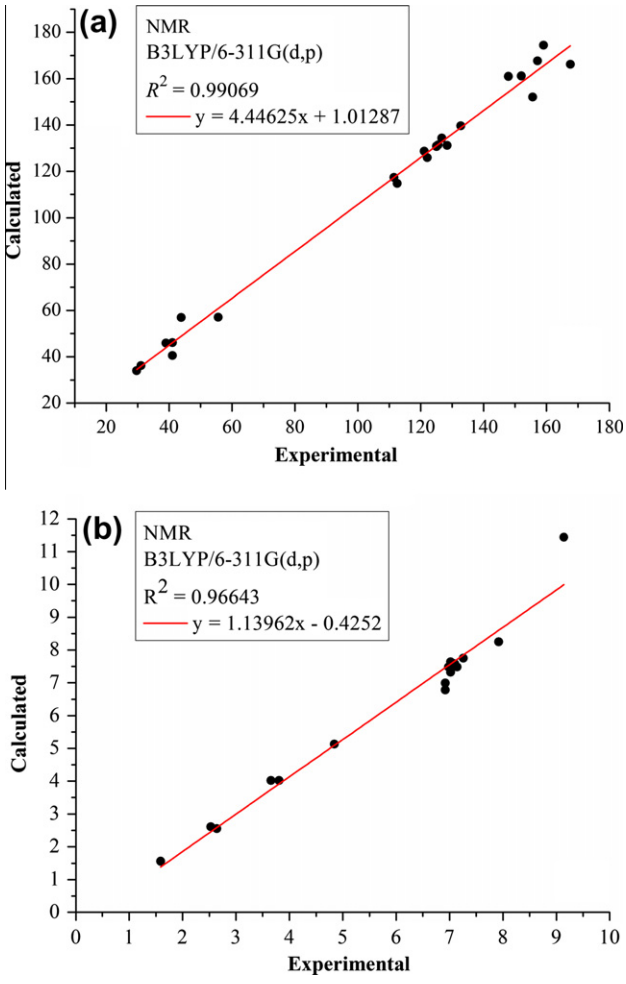

Fig. 8. Correlation graphics between the experimental and theoretical NMR chemical shift values of the title compound.

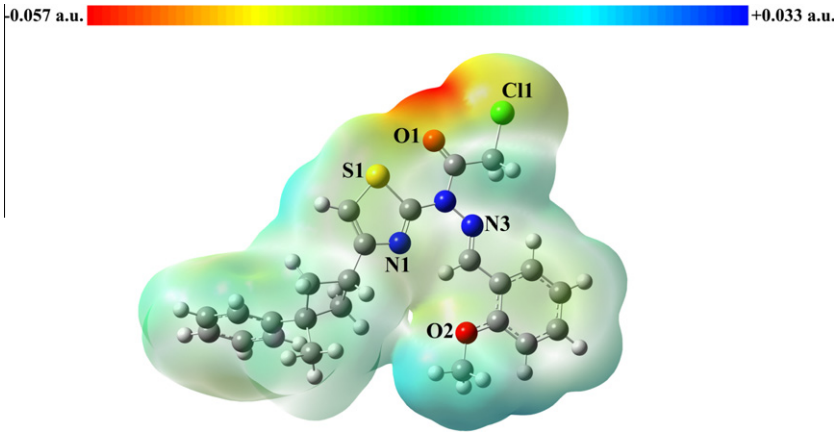

Fig. 9. Molecular electrostatic potential map calculated at B3LYP/6-311G(d,p) level.

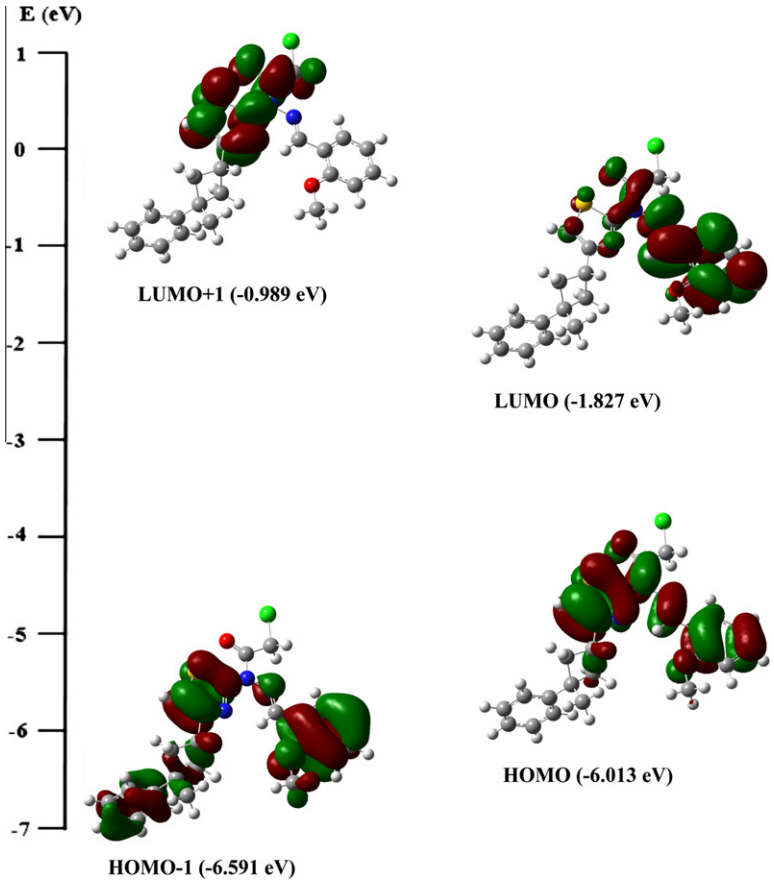

Fig. 10. Molecular orbital surfaces and energy levels given in parentheses for the HOMO − 1, HOMO, LUMO and LUMO + 1 of the title compound computed at B3LYP/6-311G(d,p) level.

To visually consider the most probable sites of the title molecule for an interaction with electrophilic and nucleophilic species, MEP was calculated at the B3LYP/6-311G(d,p) optimized geometry. While electrophilic reactivities visualized by red* color which indicate the negative regions of the molecule, the nucleophilic reactivities colored by blue, indicating the positive regions of the molecule as shown Fig. 8.

As can be seen in from Fig. 8, there is one possible site on the title compound for electrophilic attack. The negative regions are mainly over the O1 atom. But chlorine also is negative, with the characteristic negative ring and a less negative region on the extension of the bond to the chlorine atom (the σ-hole). A σ-hole is more positive as the partner in the covalent bond is more electron withdrawing. Thus, as shall be seen, in thiazole σ-hole on the extension of an S—C bond is more positive than that on the extension of an O—C bond [58]. The maximum values of negative and positive regions are −0.057 and 0.033 a.u., respectively. These results provide information concerning the region where the

* For interpretation of color in Figs. 4 and 8, the reader is referred to the web version of this article.

compound can have intra- or intermolecular interaction and metallic bonding. So, the MEP map confirms the existence of intra- and intermolecular interactions observed in the solid state.

3.6. Frontier molecular orbitals

The frontier molecular orbitals play an important role in the electric and optical properties, as well as in UV–Vis spectra and chemical reactions [59]. By examining the frontier orbitals of a molecule the optical properties and the steps to react with other molecules can be determined. The calculations indicate that the tittle compound has 119 occupied molecular orbitals.

Fig. 9 shows the distributions and energy levels of the HOMO − 1, HOMO, LUMO and LUMO + 1 orbitals computed at the B3LYP/6-311G(d,p) level for the title compound. Both the highest occupied molecular orbitals (HOMOs) and the lowest-lying unoccupied molecular orbitals (LUMOs) are mainly located at the rings and mostly the π-antibonding type orbitals. The value of the energy separation between the HOMO and LUMO is 7.84 eV. This large HOMO–LUMO gap automatically means high excitation energies for many of the excited states, good stability and a large chemical hardness for the title compound.

3.7. Conformational analysis

Based on B3LYP/6-311 G(d,p) optimized geometry for molecule A, the total energy of the title compound has been calculated by this method, which is −2102.39172692 a.u. In order to define the preferential position of the benzene ring with respect to cyclobutane ring and the preferential position of 2-chloro-*N*′-(2-methoxybenzylidene)acetohydrazide fragment with respect to thiazole ring, respectively, a preliminary search of low-energy structures was performed using AM1 computation as a function of selected torsion angles φ_1 (C6—C1—C7—C9) and φ_2 (S1—C14—N2—N3). The respective values of the selected degrees of torsional freedom, φ_1 (C6—C1—C7—C9) and φ_2 (S1—C14—N2—N3), are 127.3° and −165.3° in the X-ray structure, whereas the corresponding values in optimized geometries are 141.15° and −179.45° for B3LYP/6-311G(d,p).

Molecular energy profiles with respect to rotations about selected torsion angles are presented in Fig. 10. According to the results the low energy domains for φ_1 (C6—C1—C7—C9) are located at −40° and 140° having energy of 0.115501 and 0.115502 a.u., respectively, while they are located at −110° and 100° having energy of 0.112093 and 0.114418 a.u., respectively, for φ_2 (S1—C14—N2—N3). The energy difference between the most favorable and most unfavorable conformers, which arises from the rotational potential barrier calculated with respect to the selected torsion angle, was calculated as 0.00343 a.u. for φ_1 (C6—C1—C7—C9) and as 0.01039 a.u. for φ_2 (S1—C14—N2—N3), when both selected degrees of torsional freedom are considered (see Fig. 11).

3.8. Non-linear optical effects

Non-linear optical (NLO) effects arise from the interactions of electromagnetic fields in various media to produce new fields altered in phase, frequency, amplitude or other propagation characteristics from the incident fields [60]. NLO is at the forefront of current research because of its importance in providing the key functions of frequency shifting, optical modulation, optical switching, optical logic, and optical memory for the emerging technologies in areas such as telecommunications, signal processing, and optical interconnections [61–64].

The calculations of the mean linear polarizability (α_{tot}) and the mean first hyperpolarizability (β_{tot}) from the Gaussian output have been explained in detail previously [65], and DFT has been extensively used as an effective method to investigate the organic NLO materials [66]. The total molecular dipole moment (μ_{tot}), linear polarizability (α_{tot}) and first-order hyperpolarizability (β_{tot}) of the title compound were calculated at the B3LYP/6-311G(d,p) level. The calculated values of μ_{tot}, α_{tot} and β_{tot} are 7.8192 D, 49.9846 Å^3 and 1.9312×10^{-30} cm^5/esu. Urea is one of the prototypical molecules used in the study of the NLO properties of molecular systems. Therefore it was used frequently as a threshold value for comparative purposes. The values of μ_{tot}, α_{tot} and β_{tot} of urea are 3.53 D, 4.1446 Å^3 and 0.5883×10^{-30} cm^5/esu obtained at the same level. Theoretically, the first-order hyperpolarizability of the title compound is of 3.2 times magnitude of urea. According to these results, the title compound is a good candidate of NLO material.

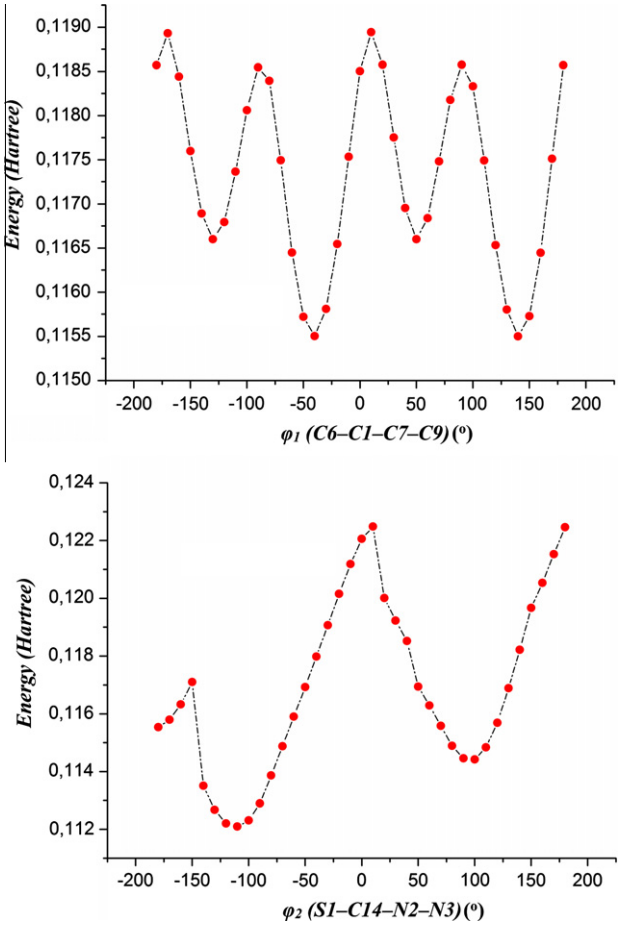

Fig. 11. Molecular energy profile of the optimized counterpart of the tittle compound versus selected degrees of torsional freedom.

4. Conclusions

In this study, *N*′-(2-methoxy-benzylidene)-*N*-[4-(3-methyl-3-phenyl-cyclobutyl)-thiazol-2-yl]-chloro-acetic hydrazide, ($C_{24}H_{24}ClN_3O_2S$), was synthesized and characterized by spectroscopic (FT-IR and NMR) and structural (single-crystal X-ray diffraction) techniques. To support the solid state structure, the geometric parameters, vibrational frequencies and ^{1}H and ^{13}C NMR chemical shifts of the title compound have been calculated using the density functional theory (DFT/B3LYP) method with the 6-311G(d,p) basis set, and compared with the experimental findings. The MEP map shows that the negative potential sites are on electronegative

atoms and the positive potential sites are around the hydrogen atoms. These sites provide information concerning the region from where the compound can undergo intra- and intermolecular interactions. The value of the energy separation between the HOMO and LUMO is very large and this energy gap gives significant information about the title compound. The predicted nonlinear optical (NLO) properties of the title compound are much greater than those of urea. The title compound is a good candidate as second-order nonlinear optical material.

Supplementary material

CCDC 815994 contains supplementary crystallographic data (excluding structure factors) for the structure reported in this article. These data can be obtained free of charge via http://www.ccdc.cam.ac.uk/data_request/cif, by e-mailing data_request@ccdc.cam.ac.uk or by contacting The Cambridge Crystallographic Data Centre, 12 Union Road, Cambridge CB2 1EZ, UK; fax: +44 1223 336033.

Acknowledgments

I wish to thank Prof. Dr. Orhan Büyükgüngör for his help with the data collection and acknowledge the Faculty of Arts and Sciences, Ondokuz Mayıs University, Turkey, for the use of the STOE IPDS II diffractometer (purchased under Grant No. F-279 of the University Research Fund).

References

[1] R. Barone, M. Chanon, R. Gallo, Aminothiazoles and Their Derivatives: The Chemistry of Heterocyclic Compounds, vol. 34, Interscience Publishers, Wiley, New York, 1979. pp. 9–366.
[2] P. Crews, Y. Kakou, E. Quinoa, J. Am. Chem. Soc. 110 (1988) 4365.
[3] H. Shinagawa, H. Yamaga, H. Houchigai, Y. Sumita, M. Sunagawa, Bioorg. Med. Chem. 5 (1997) 601.
[4] B. Shivarama Holla, K.V. Malini, B.R. Sooryanarayana, B.K. Sarojini, K.N. Suchetha, Eur. J. Med. Chem. 38 (2003) 313.
[5] G. Nam, J.C. Lee, D.Y. Chi, J.-H. Kim, Bull. Korean Chem. Soc. 11 (1990) 383.
[6] (a) U.G. Ibatullin, T.F. Petrushina, L.Y. Leitis, I.Z. Minibaev, B.O. Logvin, Khim. Geterotsikl. Soedin. (USSR) 715 (1993).;
(b) U.G. Ibatullin, T.F. Petrushina, L.Y. Leitis, I.Z. Minibaev, B.O. Logvin, Chem. Abstr. 120 (1994) 1145.
[7] E.V. Dehmlow, S. Schmidt, Liebigs Ann. Chem. 5 (1990) 411.
[8] L. Coghi, A.M.M. Lanfredi, A. Tiripicchio, J. Chem. Soc. Perkin Trans. 2 (1976) 1808.
[9] K.C. Emregul, E. Duzgun, O. Atakol, Corros. Sci. 48 (2006) 873.
[10] R. Drozdzak, B. Allaert, N. Ledoux, I. Dragutan, V. Dragutan, R. Verpoort, Coord. Chem. Rev. 249 (2005) 3055.
[11] J.L. Sesssler, P.J. Melfi, G. Dan Pantos, Coord. Chem. Rev. 250 (2006) 816.
[12] C.J. Yang, S.A. Jenekhe, Macromolecules 28 (1995) 1180.
[13] S. Destri, I.A. Khotina, W. Porzio, Macromolecules 31 (1998) 1079.
[14] M. Ggrigoras, O. Catanescu, C.I. Simonescu, Rev. Roum. Chim. 46 (2001) 927.
[15] I. Kaya, A.R. Vilayetoglu, H. Mart, Polymer 42 (2001) 4859.
[16] D.R. Larkin, J. Org. Chem. 55 (1990) 1563.
[17] J. Vanco, O. Svajlenova, E. Racanska, J. Muselik, J. Valentova, J. Trace Elem. Med. Biol. 18 (2004) 155.
[18] B. Jarzabek, B. Kaczmarczyk, D. Sek, Spectrochim. Acta, A 74 (2009) 949–954.
[19] M. Jalali-Heravi, A.A. Khandar, I. Sheikshoaie, Spectrochim. Acta, A 55 (1999) 2537.
[20] H. Ünver, A. Karakaş, A. Elmali, J. Mol. Struct. 702 (2004) 49–54.
[21] Y. Zhang, Z.J. Guo, X.Z. You, J. Am. Chem. Soc. 123 (2001) 9378.
[22] F.D. Proft, P. Geerlings, Chem. Rev. 101 (2001) 1451.
[23] G. Fitzgerald, J. Andzelm, J. Phys. Chem. 95 (1991) 10531.
[24] T. Ziegler, Pure Appl. Chem. 63 (1991) 873.
[25] J. Andzelm, E. Wimmer, J. Chem. Phys. 96 (1992) 1280.
[26] G.E. Scuseria, J. Chem. Phys. 97 (1992) 7528.
[27] R.M. Dickson, A.D. Becke, J. Chem. Phys. 99 (1993) 3898.
[28] B.G. Johnson, P.M.W. Gill, J.A. Pople, J. Chem. Phys. 98 (1993) 5612.
[29] N. Oliphant, R.J. Bartlett, J. Chem. Phys. 100 (1994) 6550.
[30] G.M. Sheldrick, SHELXS-97. Program for the Solution of Crystal Structures, University of Gö ttingen, 1997.
[31] G.M. Sheldrick, SHELXL-97. Program for Crystal Structures Refinement, University of Göttingen, 1997.
[32] L.J. Farrugia, J. Appl. Crystallogr. 30 (1999) 837.
[33] Stoe & Cie, X-AREA (Version 1.18) and X-RED32 (Version 1.04) Stoe & Cie, Darmstadt, 2002.
[34] A.L. Spek, Acta Crystallogr., D 65 (2009) 148.
[35] K. Brandenburg, DIAMOND, Demonstration Version 3.1, Crystal Impact GbR, Bonn, Germany, 2006.
[36] R. Dennington II, T. Keith, J. Millam, Gauss View, Version 4.1.2, Semichem Inc., Shawnee Mission, KS, 2007.
[37] M.J. Frisch, G.W. Trucks, H.B. Schlegel, G.E. Scuseria, M.A. Robb, J.R. Cheeseman, J.A. Montgomery Jr., T. Vreven, K.N. Kudin, J.C. Burant, J.M. Millam, S.S. Iyengar, J. Tomasi, V. Barone, B. Mennucci, M. Cossi, G. Scalmani, N. Rega, G.A. Petersson, H. Nakatsuji, M. Hada, M. Ehara, K. Toyota, R. Fukuda, J. Hasegawa, M. Ishida, T. Nakajima, Y. Honda, O. Kitao, H. Nakai, M. Klene, X. Li, J.E. Knox, H.P. Hratchian, J.B. Cross, V. Bakken, C. Adamo, J. Jaramillo, R. Gomperts, R.E. Stratmann, O. Yazyev, A.J. Austin, R. Cammi, C. Pomelli, J.W. Ochterski, P.Y. Ayala, K. Morokuma, G.A. Voth, P. Salvador, J.J. Dannenberg, V.G. Zakrzewski, S. Dapprich, A.D. Daniels, M.C. Strain, O. Farkas, D.K. Malick, A.D. Rabuck, K. Raghavachari, J.B. Foresman, J.V. Ortiz, Q. Cui, A.G. Baboul, S. Clifford, J. Cioslowski, B.B. Stefanov, G. Liu, A. Liashenko, P. Piskorz, I. Komaromi, R.L. Martin, D.J. Fox, T. Keith, M.A. Al-Laham, C.Y. Peng, A. Nanayakkara, M. Challacombe, P.M.W. Gill, B. Johnson, W. Chen, M.W. Wong, C. Gonzalez, J.A. Pople, Gaussian 03, Revision E.01, Gaussian, Inc., Wallingford, CT, 2004.
[38] K.K. Irikura, R.D. Johnson III, R.N. Kacker, J. Phys. Chem. A 109 (2005) 8430.
[39] R. Ditchfield, J. Chem. Phys. 56 (1972) 5688.
[40] K. Wolinski, J.F. Hinton, P. Pulay, J. Am. Chem. Soc. 112 (1990) 8251.
[41] E. Cancès, B. Mennucci, J. Tomasi, J. Chem. Phys. 107 (1997) 3032.
[42] P. Politzer, S.J. Landry, T. Warnheim, Phys. Chem. 86 (1982) 4767, http://dx.doi.org/10.1021/j100221a024.
[43] J.S. Murray, P. Lane, T. Brinck, P. Politzer, P. Sjoberg, J. Phys. Chem. 95 (1991) 14.
[44] D.C. Swenson, M. Yamamoto, D.J. Burton, Acta Crystallogr., C 53 (1997) 1445.
[45] A. Cukurovali, N. Özdemir, I. Yilmaz, M. Dinçer, Acta Crystallogr., E 61 (2005) o1754.
[46] F.H. Allen, Acta Crystallogr., B 40 (1984) 64.
[47] A. Bondi, J. Phys. Chem. 68 (1964) 441.
[48] J.S. Murray, P. Lane, P. Politzer, Int. J. Quantum Chem. 108 (2008) 2770.
[49] J. Bernstein, R.E. Davis, L. Shimoni, N.-L. Chang, Angew. Chem., Int. Ed. Engl. 34 (1995) 1555.
[50] F.F. Jian, P.S. Zhao, Z.S. Bai, L. Zhang, Struct. Chem. 16 (2005) 635.
[51] I. Dennington, R.T. Keith, J. Millam, K. Eppinnett, W. Hovell, GaussView Semichem, Inc., Shawnee Mission, KS, 2003.
[52] E. Scrocco, J. Tomasi, Adv. Quantum Chem. 11 (1979) 115.
[53] F.J. Luque, J.M. Lopez, M. Orozco, Theor. Chem. Acc. 103 (2000) 343.
[54] N. Okulik, A.H. Jubert, Int. Electron. J. Mol. Des. 4 (2005) 17.
[55] P. Politzer, P.R. Laurence, K. Jayasuriya, J. McKinney, Environ. Health Perspect. 61 (1985) 191.
[56] E. Scrocco, J. Tomasi, Topics in Current Chemistry, vol. 7, Springer, Berlin, 1973. p. 95.
[57] P. Politzer, D.G. Truhlar, Chemical Applications of Atomic and Molecular Electrostatic Potentials, Plenum, New York, 1981.
[58] P. Politzer, J.S. Murray, in: J. Leszczynski, M. Shukla (Eds.), Practical Aspects of Computational Chemistry, Springer, Heidelberg, 2009, p. 149. p. 149.
[59] I. Fleming, Frontier Orbitals and Organic Chemical Reactions, Wiley, London, 1976.
[60] Y.-X. Sun, Q.-L. Hao, W.-X. Wei, Z.-X. Yu, L.-D. Lu, X. Wang, Y.-S. Wang, J. Mol. Struct., THEOCHEM 904 (2009) 74.
[61] C. Andraud, T. Brotin, C. Garcia, F. Pelle, P. Goldner, B. Bigot, A. Collet, J. Am. Chem. Soc. 116 (1994) 2094.
[62] V.M. Geskin, C. Lambert, J.L. Bredas, J. Am. Chem. Soc. 125 (2003) 15651.
[63] M. Nakano, H. Fujita, M. Takahata, K. Yamaguchi, J. Am. Chem. Soc. 124 (2002) 9648.
[64] D. Sajan, H. Joe, V.S. Jayakumar, J. Zaleski, J. Mol. Struct. 785 (2006) 43.
[65] K.S. Thanthiriwatte, K.M. Nalin de Silva, J. Mol. Struct., THEOCHEM 617 (2002) 169.
[66] Y.-X. Sun, Q.-L. Hao, Z.-X. Yu, W.-X. Wei, L.-D. Lu, X. Wang, Mol. Phys. 107 (2009) 223.